

## New Giant Dipole Strength in ${}^6\text{Li}$ and ${}^7\text{Li}$ as Revealed via $(n,p)$ at 60 MeV

F. Brady, G. A. Needham,<sup>(a)</sup> J. L. Romero, C. M. Castaneda, T. D. Ford,  
J. L. Ullmann,<sup>(b)</sup> and M. L. Webb

*Department of Physics and Crocker Nuclear Laboratory, University of California, Davis, California 95616*

(Received 31 January 1983)

The  $(n,p)$  reaction in  ${}^6\text{Li}$  and  ${}^7\text{Li}$  at 60 MeV reveals large structures at high excitations which are the analogs of states in  ${}^6\text{Li}$  and  ${}^7\text{Li}$  at 29 and 31 MeV, respectively. These new structures, which exhibit giant dipole strength, are not seen in photoneutron data. They do not appear to contain appreciable dipole spin-mode strength. The exhaust large sum-rule fractions, and largely answer the longstanding question of missing giant dipole resonance strength in these nuclei.

PACS numbers: 25.40.Fq, 24.30.Cz

The giant dipole resonance (GDR) is one of the outstanding manifestations of collective phenomena in nuclei. Mainly its study has been carried out via photonuclear and particle-capture reactions. However, recently inelastic electron and hadron scattering have been used to study the GDR and other modes of collective motion in nuclei. A disadvantage with these reactions is that they excite both isovector and isoscalar transitions. The result is that the GDR, which is of isovector nature, tends to be obscured and/or overlapped by strong isoscalar electric quadrupole and monopole resonances.

The charge-exchange reactions such as  $(p,n)$  and  $(n,p)$  offer a powerful option to isolate the isovector modes such as the GDR in that they excite the isovector analogs in isobars of the target. In the case of the GDR in very light nuclei there has been longstanding evidence that only a fraction ( $\cong 30\%$ ) of the classical Thomas-Reich-Kuhn (TRK) dipole sum rule is exhausted in photoneutron reaction measurements.<sup>1</sup> We have studied  ${}^6\text{Li}$  and  ${}^7\text{Li}$  targets using the  $(n,p)$  reaction at 60 MeV and find at high excitation large enhancements which have  $l=1$  character, and so appear to be analogs of large fragments of the missing GDR.

To measure  $(n,p)$  we used our new detection system<sup>2</sup> consisting of multiwire chambers (MWC's) to give the trajectories of the outgoing charged particles, and large-area NE102 plastic  $\Delta E$  and NaI  $E$  detectors to provide large detection solid angles. The neutron facility has been described elsewhere.<sup>3,4</sup> The 60-MeV neutron beam, produced by  ${}^7\text{Li}(p,n)$  at  $0^\circ$ , is collimated to form a  $1.8 \times 3.6\text{-cm}^2$  beam spot of intensity  $10^6$  neutrons/sec for 1-MeV full width at half maximum neutron peak. A neutral  $\text{H}^0$  beam which can pass through the proton clearing magnet is useful for calibrating the system.<sup>5</sup> The

${}^6\text{Li}$  and  ${}^7\text{Li}$  targets were  $>99\%$  pure isotopically, and about 600 keV thick for protons. The  $n+p$  cross section, measured separately with a  $\text{CH}_2$  target, provided an absolute normalization.

Figure 1 shows the angle-integrated ( $6.5^\circ$  to  $32.5^\circ$ —the interval which contains the peak in the dipole angular distribution) energy spectra for  ${}^6\text{Li}$  and  ${}^7\text{Li}$  (top). The striking features are the large structures at higher excitations. The (arbitrarily normalized)  ${}^6\text{Li}(\gamma, xn)$  photonuclear data<sup>1,6</sup> are shown as referred to the  ${}^6\text{Li}$  excitation energy scale. The  $(\gamma, xn)$  includes  $(\gamma, n)$ ,  $(\gamma, np)$ ,  $(\gamma, nd)$ , and  $(\gamma, n2p)$ , and up to  $E_\gamma \cong 21$  MeV also includes  $(\gamma, p)$  because in this energy range  ${}^5\text{He}$  decays solely to  ${}^4\text{He}+n$ . The  $(\gamma, xn)$  measurements show a broad peak at  $E_x \cong 12$  MeV in  ${}^6\text{Li}$  ( $E_x \cong 8.5$  MeV for the analog in  ${}^6\text{He}$ ), but show little evidence for the analogs of the structures near 15.5 and 25 MeV in  ${}^6\text{He}$ . ( $E_x \cong 19$  and 28.5 MeV are the analog energies in  ${}^6\text{Li}$ .) The solid curve labeled  $P$  is an angle-integrated prediction for the continuum from the preequilibrium model PRECO-B.<sup>7</sup> Its absolute value is not predicted very accurately and so it is normalized to the data at high excitation energies.

Angle-by-angle cross sections for enhancements above the continuum (inferred from the shape of the angle-integrated prediction) were obtained by fitting the continuum-subtracted data with Gaussians. Within statistical fluctuations these enhancements retain their shapes and the centroids track well from angle to angle when two-body kinematics are assumed in the final state.

The lines above the spectrum at 15.5 and 23.2 MeV in  ${}^6\text{He}$  show where evidence for broad excitations,  $\Gamma = 1.7 \pm 2.0$ ,  $\Gamma = 4.0 \pm 3.1$ , respectively, has been reported<sup>8</sup> in  ${}^6\text{Li}(\pi^-, \gamma){}^6\text{He}$ . Possible states at  $13.4 \pm 0.5$  ( $\Gamma = 1.2$  MeV) and at  $15.3 \pm 0.3$  MeV were reported<sup>9</sup> in  ${}^7\text{Li}(p, 2p)$  at 156 MeV.

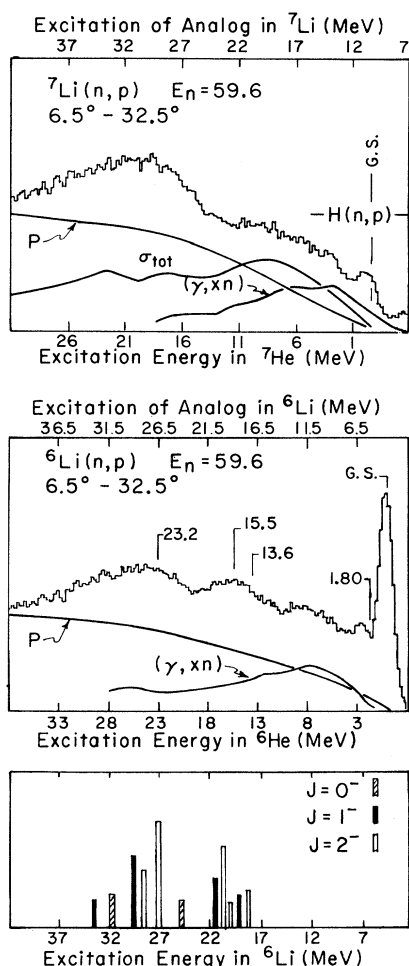


FIG. 1. Angle-integrated  $(n, p)$  spectra for  ${}^6\text{Li}$  and  ${}^7\text{Li}$ . The vertical lines above the  ${}^6\text{Li}(n, p)$  spectrum indicate energies at which evidence for (narrower) resonances has been observed. The bottom figure is a shell-model calculation of GDR strength for  ${}^6\text{Li}$  as referred to in the text.

Later<sup>10</sup> higher-statistics data at 100 MeV indicated just one broad bump ( $\Gamma = 4$  MeV) at about 14 MeV. The state that we observe at  $15.5 \pm 0.5$  MeV in  ${}^6\text{He}$  is broad,  $\Gamma = 6 \pm 1.5$  MeV; and the large structure at higher excitation,  $25 \pm 1$  MeV, is also broad,  $\Gamma = 8 \pm 2$  MeV.

In the  ${}^7\text{Li}(n, p){}^7\text{He}$  spectrum (Fig. 1) the ground state in  ${}^7\text{He}$  is at  $-Q(n, p) = 10.4$  MeV and the analog in Li is placed<sup>11</sup> at  $E_x = 11.24$  MeV. The hydrogen contamination is from oil which apparently was not completely removed from the target. The H contribution seen above the ground-state peak tails off rapidly towards the kinematic limit at  $E_{c.m.} \approx 36$  MeV in Fig. 1, and that from C, assuming  $\text{CH}_2$  for the oil, is small, only  $\approx 1\%$

of the spectrum.

A large enhancement is seen centered at  $E_x = 20 \pm 1$  MeV in  ${}^7\text{He}$  with a width  $\Gamma \approx 9 \pm 2$  MeV. The analog in Li will be at  $E_x \approx 31$  MeV. There is also evidence for a broad enhancement centered near 6 MeV in  ${}^7\text{He}$  which corresponds to approximately the same energy centroid,  $E_x \approx 17$  MeV in  ${}^7\text{Li}$ , as the peak of the enhancement seen in  $(\gamma, xn)$  photonuclear cross sections.<sup>12</sup> However the  $(\gamma, xn)$  decreases monotonically as one goes to higher excitation and does not indicate even the beginning of the enhancement centered near 31 MeV excitation in  ${}^7\text{Li}$ . The total photonuclear cross sections<sup>13</sup> for  ${}^7\text{Li}$  do show more strength at higher  $E_x$  and fall off slowly with  $E_x$  in  ${}^7\text{Li}$ . These are shown as the line  $\sigma_{\text{tot}}$  in Fig. 1 which was taken from Ref. 13. They show possible evidence for structure, which has a double bump, over the energy range that  $(n, p)$  shows the 31-MeV structure. The selection rule  $\Delta T_3 = \Delta T = +1$  means that only analogs of isospin  $T = T_0 + 1 = \frac{3}{2}$  states of  ${}^7\text{Li}$  (and not  $T = \frac{1}{2}$ ) will be excited in  $(n, p)$ . However, the photonuclear process will excite both  $T_0$  and  $T_0 + 1$  states and this could account for the differences between  $(n, p)$  and  $\sigma_{\text{tot}}$ .

Figure 2 shows the angular distributions (top) for the structures at 15.5 and 25 MeV in  ${}^6\text{He}$ , and (bottom) for the 20-MeV structure in  ${}^7\text{He}$ . The Goldhaber-Teller<sup>14</sup> (GT) model (which is deemed the most appropriate model of the GDR in light nuclei<sup>15</sup>) was used to provide a macroscopic form factor<sup>16</sup> for distorted-wave Born-approximation calculations using DWUCK IV.<sup>17</sup> Satchler's model<sup>16</sup> has been generalized<sup>18</sup> to include isospin and be applicable to  $(n, p)$ . A  $p$ -shell optical model<sup>19</sup> was used and provided good fits to the ground-state transitions in  ${}^6\text{Li}$  and  ${}^7\text{Li}(n, p)$ .<sup>2</sup> For the excited states only the fits using  $l(\text{transfer}) = 1$  are reasonable and the results assuming  $l = 1$ ,  $s(\text{transfer}) = 0$  are that the structure at 15.5 MeV in  ${}^6\text{He}$  exhausts  $\approx 24\%$  and that at 25 MeV,  $\approx 46\%$  of the GT energy-weighted sum rule (EWSR). The broad structure at lower excitation,  $\approx 7$  MeV in  ${}^6\text{He}$  (Fig. 1), contributes  $\approx 15\%$  of the GT EWSR in the  $(n, p)$  case. Thus about 85% of the GT EWSR is exhausted for excitations up to  $\approx 35$  MeV in  ${}^6\text{Li}$ . This can be compared with the TRK energy-integrated sum-rule fraction of  $\approx 33\%$  (Ref. 1).

In the case of  ${}^7\text{Li}$ , using the GT form factor, and assuming  $s = 0$ , one finds that the enhancement at  $E_x \approx 20$  MeV in  ${}^7\text{He}$  exhausts about 70% of the GT EWSR. In the lower excitation-energy region, that of the  $(\gamma, xn)$  peak, only about 24%

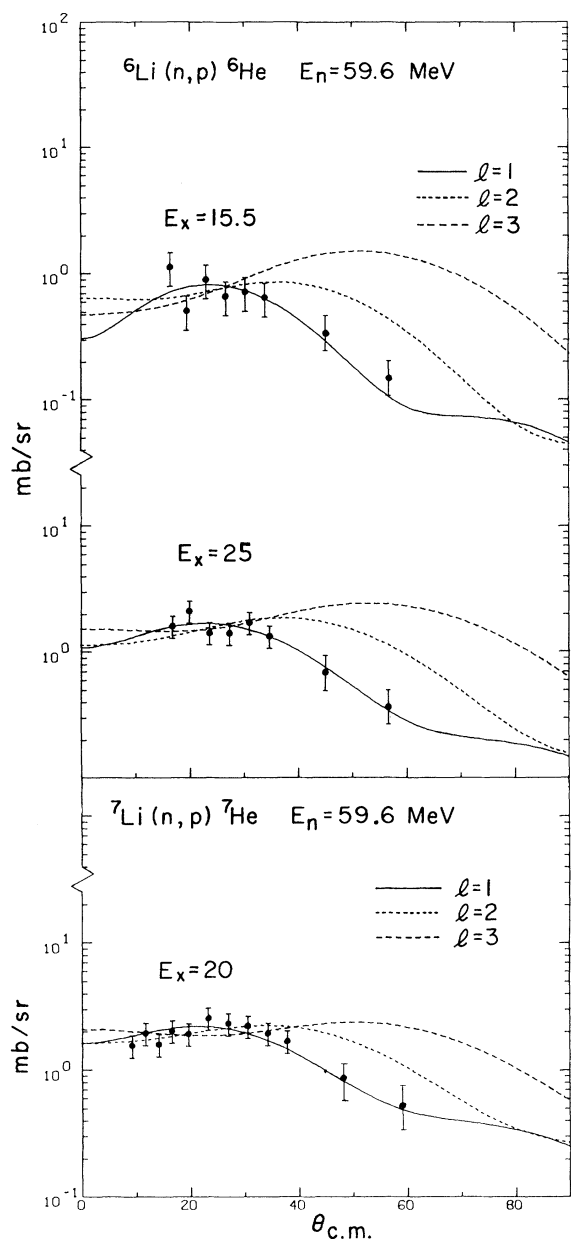


FIG. 2. Differential cross sections for the 15.5- and 25-MeV structures in  ${}^6\text{He}$  and for the 20-MeV structure in  ${}^7\text{He}$ , compared with distorted-wave Born-approximation calculations using a Goldhaber-Teller macroscopic form factor.

of the GT EWSR is accounted for in the  $(n, p)$  spectrum. So a total of  $\approx 94\%$  of the EWSR in  ${}^7\text{Li}$  is accounted for. These sum-rule fractions are uncertain to  $\approx 20\%$  because of uncertainties in fitting  $\sigma(\theta)$ , in the  $n + \text{H}$  normalization, and in the continuum subtraction.

Although the application of collective-model

sum rules to very light nuclei is not well tested or considered to be very quantitative, results for other light nuclei (C, N, and O) have been very reasonable.<sup>2,18</sup> The point here is that these excitations at high energy in  ${}^6\text{Li}$  and  ${}^7\text{Li}$  do contain large fractions of the EWSR, and would add to and more than double the total TRK sum-rule fractions of  $\approx 30\%$  for  $(\gamma, xn)$  energy integrated to 35 MeV.

The photonuclear GDR has  $s=0$ . However, we cannot determine the spin transfer from the data. It is estimated that the isovector spin-flip component of the nucleon-nucleon interaction at 60 MeV is comparable in strength to the spin-independent component.<sup>20</sup> A way of localizing spin-flip strength is via the  $(d, {}^2\text{He})$  reaction, which involves both spin and isospin transfer (of one unit in each case). A comparison of  ${}^6\text{Li}(d, {}^2\text{He}){}^6\text{He}$  (Ref. 21) and  ${}^6\text{Li}(n, p){}^6\text{He}$  at comparable momentum transfers shows little or no evidence for the structures seen in the  $(n, p)$  at  $E_x({}^6\text{He}) \approx 15.5$  and 25 MeV. For other light nuclei<sup>3,22</sup> ( ${}^{12}\text{C}$ ,  ${}^{16}\text{O}$ ) a large fraction of the spin-transfer dipole ( $l=1, s=1$ ) strength also seems to be quenched, or greatly fragmented. Calculations<sup>23</sup> also show that spin-flip strength is proportional to the final number of substates of a given  $J$  ( $2J+1$ ) with the highest spin states lowest in energy. No such concentration is seen here. At this time we can only make a qualitative statement that at least for  ${}^6\text{Li}$  the  $s=1, l=1$  mode is small or is so fragmented in energy that it cannot be seen. In the case of  ${}^7\text{Li}$ ,  $(d, {}^2\text{He})$  is not available, but 200-MeV  $(p, n)$  data<sup>24</sup> which excite the spin modes do not show this high-energy structure.

The fact that the analogs of the structures at 15.5 and 25 MeV in  ${}^6\text{He}$  (20.0 and 29.5 MeV in  ${}^6\text{Li}$ ) and at 20 MeV in  ${}^7\text{He}$  (31 MeV in  ${}^7\text{Li}$ ) are not seen in  $(\gamma, xn)$  seems to indicate that they have important decay modes which do not produce neutrons. In fact the study of  ${}^6\text{Li}(\gamma, t){}^3\text{He}$  (Ref. 25) and the inverse reaction<sup>26,27</sup> shows that this two-body channel is important and contributes 20% of the TRK sum rule up to  $E_\gamma=32$  MeV.<sup>27</sup> The inferred  $(\gamma, t)$  cross section peaks at  $E_\gamma \approx 19.5$  MeV and by  $E_\gamma \approx 30$  MeV has decreased monotonically to 0.3 that at the peak. There is no evidence in the two-body data for an additional structure centered near 29.5 MeV whose analog is prominent in  $(n, p)$ . This suggests that the 29.5-MeV structure may decay largely into  ${}^3\text{H} + p + d$ . In fact, the analog resonance at 29.5 MeV in  ${}^6\text{Li}$  begins near 22 MeV

( ${}^6\text{Li}$  excitation), which is near the thresholds for  ${}^6\text{Li}(\gamma, {}^3\text{He})d+n$  and  $(\gamma, {}^3\text{H})d+p$ . Decay of the resonance into the latter outgoing channel produces no neutrons. The 31-MeV structure in  ${}^7\text{Li}$  begins near  $\cong 23$  MeV which is close to the threshold, 22.3 MeV, for  ${}^3\text{H}+t+p$  decay of  ${}^7\text{Li}$  (excited) which also produces no neutrons.

Shell-model calculations of GDR strength<sup>28</sup> ( $l=1, s=0$ ) in  ${}^6\text{Li}$  show strength in the range 17.9 to 33.7 MeV (the bars in Fig. 1, bottom) with the main  $2^-$  components at 20.8 and 27.0 MeV, the largest  $1^-$  at 21.3 and 29.4, and the  $0^-$  of lesser strength and fragmented. ( ${}^6\text{Li}$  has a  $1^+$  ground state.) In these calculations  $1s_{1/2}$  hole configurations play a large role. An earlier calculation<sup>29</sup> shows a similar distribution of strength. As can be seen in Fig. 1 the predictions<sup>28</sup> are not far off the experimental energies of  $20 \pm 1$  and  $29.5 \pm 1$  MeV excitation in  ${}^6\text{Li}$ , which are inferred from these  $(n, p)$  measurements.

One concludes that at high excitations, 29.5 MeV in  ${}^6\text{Li}$  and 31 MeV in  ${}^7\text{Li}$ , large  $l=1$  structures exist which are not evident in photoneutron cross sections, but which exhaust large dipole sum-rule fractions. These structures do not appear to contain appreciable dipole spin-mode components.

We acknowledge the support of National Science Foundation Grant No. PHY-79-26282 and the assistance of Crocker Nuclear Laboratory and Physics Department staff. We also thank Dr. George Bertsch for helpful comments.

<sup>(a)</sup>Present address: Rocketdyne Division, Rockwell International, Canoga Park, Cal. 91304.

<sup>(b)</sup>Present address: Nuclear Physics Laboratory, University of Colorado, Boulder, Colo. 80309.

<sup>1</sup>B. L. Berman and S. C. Fultz, *Rev. Mod. Phys.* **47**, 713 (1975).

<sup>2</sup>G. A. Needham, Ph.D. thesis, University of California, Davis, 1981 (unpublished).

<sup>3</sup>F. P. Brady and G. A. Needham, in *The (p, n) Reaction and the Nucleon-Nucleon Force*, edited by C. D. Goodman *et al.* (Plenum, New York, 1980), p. 357, and references therein. N. S. P. King and J. L. Ullmann, *ibid.*, p. 373.

<sup>4</sup>J. A. Jungerman and F. P. Brady, *Nucl. Instrum.*

*Methods* **89**, 167 (1970); J. L. Romero, T. S. Subramanian, F. P. Brady, N. S. P. King, and J. F. Harrison, in *Proceedings of the Symposium on Neutron Cross Sections*, edited by M. R. Bhat and S. Pearlstein, BNL Report No. BNL-NCS-50681, 1977 (unpublished).

<sup>5</sup>J. L. Romero *et al.*, *Nucl. Instrum. Methods* **171**, 609 (1980).

<sup>6</sup>B. L. Berman, R. L. Bramblett, J. T. Caldwell, R. R. Harvey, and S. C. Fultz, *Phys. Rev. Lett.* **15**, 727 (1965).

<sup>7</sup>PRECO-B was written by C. Kalbach (unpublished).

<sup>8</sup>H. W. Baer *et al.*, *Phys. Rev. C* **8**, 2029 (1973).

<sup>9</sup>J. C. Roynette, M. Arditì, J. C. Jacmart, F. Mazlaum, M. Riou, and C. Ruhla, *Nucl. Phys.* **A95**, 545 (1967).

<sup>10</sup>R. K. Blomwick, C. C. Chang, J. P. Didelez, and H. D. Holmgren, *Phys. Rev. C* **13**, 2105 (1976).

<sup>11</sup>F. Ajzenberg-Selove, *Nucl. Phys.* **A320**, 1 (1979).

<sup>12</sup>R. L. Bramblett, B. L. Berman, M. A. Kelly, J. T. Caldwell, and S. C. Fultz, in *Proceedings of the International Conference on Photoneuclear Reactions and Applications, Pacific Grove, 1973*, edited by B. L. Berman (Lawrence Livermore Laboratory, Livermore, Calif., 1973), p. 175.

<sup>13</sup>J. Ahrens *et al.*, *Nucl. Phys.* **A251**, 479 (1975).

<sup>14</sup>M. Goldhaber and E. Teller, *Phys. Rev.* **74**, 1046 (1948).

<sup>15</sup>W. D. Myers, W. J. Swiatecki, T. Kadoma, L. J. El-Jaick, and E. R. Hilf, *Phys. Rev. C* **15**, 2032 (1977).

<sup>16</sup>G. R. Satchler, *Nucl. Phys.* **A195**, 1 (1972).

<sup>17</sup>DWUCK IV computer program by P. D. Kunz, Nuclear Physics Laboratory, University of Colorado (unpublished).

<sup>18</sup>G. A. Needham *et al.*, *Nucl. Phys.* **A385**, 349 (1982).

<sup>19</sup>B. A. Watson, P. P. Singh, and R. E. Segel, *Phys. Rev.* **182**, 977 (1969).

<sup>20</sup>T. N. Taddeuci *et al.*, *Phys. Rev. C* **25**, 1094 (1982).

<sup>21</sup>D. P. Stahel, R. Jahn, G. J. Wozniak, and Joseph Cerny, *Phys. Rev. C* **20**, 1680 (1980).

<sup>22</sup>F. P. Brady, V. R. Brown, C. M. Castaneda, C. H. Poppe, and J. L. Romero, in *Proceedings of the International Conference on Spin Excitations in Nuclei, Tel-luride, 1982*, edited by F. Petrovich (to be published).

<sup>23</sup>G. Bertsch, D. Cha, and H. Toki, *Phys. Rev. C* **24**, 533 (1981).

<sup>24</sup>J. Rapaport, private communication.

<sup>25</sup>Y. M. Shin, O. M. Skopik, and J. J. Murphy, *Phys. Lett.* **55B**, 297 (1975).

<sup>26</sup>S. L. Blatt, A. M. Young, S. C. Ling, K. S. Moon, and C. D. Porterfield, *Phys. Rev.* **176**, 1148 (1968).

<sup>27</sup>E. Ventura, C. C. Chang, and W. E. Meyerhof, *Nucl. Phys.* **A173**, 1 (1971).

<sup>28</sup>J. P. Vergados, *Nucl. Phys.* **A239**, 271 (1975).

<sup>29</sup>B. S. Cooper and I. M. Eisenberg, *Nucl. Phys.* **A114**, 184 (1968).